First observations of volcanic eruption clouds from the L1 Earth-Sun Lagrange point by DSCOVR/EPIC

S. A. Carn[1,*], N. A. Krotkov[2], B.L. Fisher[2,3], C. Li[2,4], and A.J. Prata[5]

[1]Department of Geological and Mining Engineering and Sciences, Michigan Technological University, Houghton, MI 49931, USA; scarn@mtu.edu

[2]Atmospheric Chemistry and Dynamics Laboratory, Code 614, NASA Goddard Space Flight Center, Greenbelt, MD 20771, USA

[3]Science Systems and Applications, Inc. (SSAI), Lanham, MD, USA

[4]Earth System Science Interdisciplinary Center, University of Maryland, College Park, MD, USA

[5]AIRES Pty Ltd, Melbourne, Australia

*Corresponding author

Key points

- Volcanic eruption clouds can be detected and tracked with hourly temporal cadence from L1 orbit.
- The hourly cadence of EPIC volcanic SO_2 observations can be used to attribute gas emissions to specific events during multi-phase eruptions.
- Observations of transient variations in SO_2 loading will provide more constraints on processes such as H_2S oxidation in volcanic clouds.

This article has been accepted for publication and undergone full peer review but has not been through the copyediting, typesetting, pagination and proofreading process which may lead to differences between this version and the Version of Record. Please cite this article as doi: 10.1029/2018GL079808

Abstract

Volcanic sulfur dioxide (SO_2) emissions have been measured by ultraviolet (UV) sensors on polar-orbiting satellites for several decades, but with limited temporal resolution. This precludes studies of key processes believed to occur in young (~1-3 hours old) volcanic clouds. In 2015, the launch of the Earth Polychromatic Imaging Camera (EPIC) aboard the Deep Space Climate Observatory (DSCOVR) provided an opportunity for novel observations of volcanic eruption clouds from the first Earth-Sun Lagrange point (L1). The L1 vantage point provides continuous observations of the sunlit Earth, offering up to 8 or 9 observations of volcanic SO_2 clouds in the EPIC field of view at ~1 hour intervals. Here, we demonstrate EPIC's sensitivity to volcanic SO_2 using several volcanic eruptions from the tropics to mid-latitudes. The hourly cadence of DSCOVR/EPIC observations permits more timely measurements of volcanic SO_2 emissions, improved trajectory modeling, and novel analyses of the temporal evolution of volcanic clouds.

1. Introduction

Most Earth observation from space is currently performed using satellites in polar (low Earth, LEO) or geostationary (GEO) orbit. LEO sensors can provide high spatial resolution (meter-scale or better) observations, and global coverage including the polar regions at low (~daily) temporal frequency. GEO sensors offer high temporal resolution (~minutes), but lower spatial resolution (km-scale) and coverage of one hemisphere from low- to sub-polar latitudes. Hence, GEO orbits support time-critical applications (e.g., monitoring of severe weather) but LEO orbits are needed for global coverage and analyses requiring high spatial resolution.

Both LEO and GEO orbits are used for the detection and mapping of volcanic eruption clouds, with two primary goals: detection and characterization of volcanic ash

clouds for aviation safety (mainly GEO; e.g., *Pavolonis et al*., 2013), and measurement of sulfur dioxide (SO_2) emissions to assess volcanic impacts on the atmosphere and climate (mainly LEO; e.g., *Carn et al*., 2016). Although some operational GEO thermal infrared (TIR) imagers can detect volcanic SO_2 (e.g., *Prata and Kerkmann*, 2007), most SO_2 measurements are collected from LEO ultraviolet (UV) and TIR sensors, with low temporal resolution. This has limited studies of several processes that may impact the sulfur burden in fresh volcanic clouds during the first few hours of atmospheric residence, including the interaction of ash, ice (or hydrometeors) and gas, emission and oxidation of other sulfur gas species (e.g., hydrogen sulfide, H_2S), and early (or primary) sulfate aerosol formation (e.g., *Rose et al*., 2000). *Rose et al.* (2000) noted that detailed evaluation of such processes required improved data frequency, especially in the UV.

The 2015 deployment of the Earth Polychromatic Imaging Camera (EPIC) aboard the Deep Space Climate Observatory (DSCOVR), located at the first Earth-Sun Lagrange point (L1) ~1.5 million kilometers from Earth, provides a rare opportunity to explore a new Earth observation paradigm. The L1 vantage point enables a continuous view of the sunlit face of the Earth during its daily rotation. EPIC is a 10-channel UV – near IR (NIR) spectroradiometer that provides sunrise-to-sunset Earth observations with a temporal cadence of 68-110 minutes depending on season (http://epic.gsfc.nasa.gov); the highest temporal resolution of UV satellite measurements achieved to date. Calibrated EPIC radiances are available for retrievals of atmospheric trace gases including ozone (O_3) and SO_2 (*Herman et al.*, 2018; *Marshak et al.*, 2018). EPIC provides coverage of the entire sunlit Earth disk (including the polar regions in the summer months, unlike GEO sensors), partly fills a ~4-hour daytime measurement gap between overpasses of Sun-synchronous LEO assets at ~9:30 am (e.g., the European MetOp-A/B satellites) and ~1:30 pm local time (e.g., NASA's Aqua, Aura and Suomi-NPP satellites), and also collects data later into the afternoon. Here, we

present the first EPIC retrievals of SO_2 columns following several recent volcanic eruptions (Table 1) and demonstrate the potential of these unique observations to advance our understanding of volcanic cloud processes and impacts. We highlight several key advantages of observations from L1, including more timely eruption detection; improved constraints on initial eruptive SO_2 mass loading; and the potential for characterization of short-term trends in eruption intensity.

2. The EPIC instrument

EPIC is a UV-NIR spectroradiometer that captures 10 spectral exposures (using narrowband filters at wavelengths of 317.5, 325, 340, 388, 443, 551, 680, 688, 764 and 779.5 nm) of the sunlit Earth disk approximately every hour (mid-April to mid-October) or every two hours (rest of the year) using a 2048×2048 pixel Charge Coupled Device (CCD) detector with a maximum signal-to-noise ratio of 290:1 (*Herman et al.*, 2018). The spectral resolutions (full widths at half maximum) of the four UV filters (317.5-388 nm) are 1.0, 1.0, 2.7 and 2.6 nm, respectively. In the UV channels, CCD pixels are binned to yield an effective image size of 1024×1024 pixels, corresponding to a ground pixel size of about 18×18 km^2 near the image center. EPIC uses rotating filter wheels to select wavelengths, with a 30 second time lag between each exposure that means individual channels are not co-located. A correction procedure is applied to the EPIC Level 1b radiances to adjust the channel images to a common latitude-longitude grid with an accuracy of 1/4 of a pixel (*Herman et al.*, 2018). Daily EPIC images of Earth are available on the EPIC website (http://epic.gsfc.nasa.gov), where the geographical extent of the data throughout the year can be seen.. *Herman et al.* (2018) and *Marshak et al.* (2018) provide more details on the EPIC characteristics and its applications.

3. The EPIC SO_2 algorithm

We have developed a discrete band backscattered UV (BUV) SO_2 algorithm (MS_SO2) that provides consistent SO_2 retrievals across the multiple UV satellite missions deployed since the first Total Ozone Mapping Spectrometer (TOMS; *Krueger et al.*, 1995; *Krueger et al.*, 2000). In the EPIC version of MS_SO2, the four EPIC UV channels (centered at wavelengths [λ] of 317.5, 325, 340 and 388 nm) are used to retrieve a state vector containing four atmospheric parameters: SO_2 column, O_3 column, the scene reflectivity (R) at 388 nm (which assumes that the observed radiance is Lambertian, or independent of viewing angle) and the spectral reflectivity dependence, dR/dλ.

The retrieval is performed in two steps, referred to here as Step 1 and Step 2. In Step 1, the 4-element state vector, **x**, is retrieved by inverting a 4×4 weighting matrix, K:

$$\boldsymbol{y} = K\mathbf{x} \tag{1}$$

where **y** is a 4-element vector containing the four measured UV radiances. The weighting coefficients $K_{i,j}$, are defined by the respective sensitivities (or Jacobians) computed from a forward radiative transfer (RT) model for each state variable x_j:

$$K_{i,j} = \frac{\partial N_i}{\partial x_j}. \tag{2}$$

where N_i is the forward model calculated N-value (N = -100 $\log_{10}$ [I/F], where I = Top of Atmosphere radiance and F = incoming solar irradiance) at each of the four UV wavelengths, i. To calculate the SO_2 sensitivities ($\partial N/\partial SO_2$), we assume the SO_2 plume has a Gaussian vertical profile centered at 13 km altitude with a standard deviation of 2 km.

The EPIC channel geolocation errors described above produce noise in the Step 1 retrievals, which we correct for by implementing a Step 2 procedure. In Step 2, we first apply a 31×31 mean filter to smooth the entire Step 1 retrieved O_3 field, and then perform a second retrieval using the Step 1 retrieved quantities as first guesses. The O_3 and reflectivity remain

fixed in Step 2, resulting in a 2-parameter retrieval of SO_2 and $dR/d\lambda$. A UV Aerosol Index (AI) sensitive to volcanic ash, which can also be used to detect volcanic eruptions (e.g., Table 1), is calculated as: $AI = dR/d\lambda * dN/dR * (N_{340}-N_{388})$.

As we demonstrate below, the EPIC SO_2 algorithm has adequate sensitivity to detect moderate to large volcanic eruptions (Table 1) when the SO_2 column in an EPIC pixel exceeds ~5-15 Dobson Units (1 DU = 2.68×10^{16} molecules/cm^2). Although hyperspectral UV instruments such as the Ozone Monitoring Instrument (OMI) and Ozone Mapping and Profiler Suite (OMPS) have higher SO_2 sensitivity (e.g., *Carn et al.*, 2016), the EPIC observations have the benefit of higher cadence. There are several potential sources of error on the EPIC SO_2 retrievals, including aerosols (e.g., volcanic ash or sulfate aerosol) and an incorrect SO_2 altitude. RT calculations suggest maximum errors of ±30% for SO_2 plumes located within ±2 km of the assumed altitude (13 km), with larger errors at high latitudes. Potential errors due to high aerosol loadings have not yet been assessed, but could be significant in fresh, ash-rich eruption clouds.

4. Results

No major (stratospheric) eruptions have occurred since June 2015. However, there have been several smaller eruptions from equatorial (Galápagos Islands, Ecuador) to high latitudes (Alaska), permitting evaluation of EPIC's sensitivity to common volcanic events under a range of observing conditions (Table 1). To date a maximum of 8-9 EPIC consecutive exposures of a volcanic SO_2 cloud in ~8 hours has been achieved, after the eruption of Sierra Negra (Galápagos Islands, Ecuador) in June 2018. Several other eruptions have been captured in 4-7 EPIC exposures (Table 1). Here, we focus on three recent eruptions that demonstrate the advantages of these high-cadence UV observations from L1: the May 2017 eruption of

Bogoslof (Alaska, USA), the October 2017 eruption of Tinakula (Solomon Islands) and the June 2018 eruption of Sierra Negra.

4.1 The May 28-29, 2017 eruption of Bogoslof (AK, USA)

Bogoslof (AK, USA; 53.93ºN, 168.03ºW) is a largely submarine volcano in the Aleutian Islands that produced a series of 64 explosive eruptions between December 2016 and August 2017 (http://www.avo.alaska.edu). At least two of these eruptions (March 8 and May 28, 2017) were detected by EPIC (Table 1). The May 28, 2017 eruption began at 22:16 UTC (14:16 AKDT) and lasted 50 minutes, injecting a volcanic ash cloud to altitudes of at least 12 km (a Volcanic Explosivity Index [VEI] of 3; *Global Volcanism Program*, 2013) and generating significant volcanic lightning detected by the World Wide Lightning Location Network (WWLLN) at 22:40 – 23:01 UTC. As expected for a partly submerged vent, the initial eruption column was observed to be very water-rich in visible satellite imagery (e.g., https://avo.alaska.edu/images/image.php?id=109261), raising the possibility of SO_2 scavenging and/or rapid sulfate aerosol production in the volcanic plume.

Volcanic SO_2 emitted by the Bogoslof eruption was captured in 4 EPIC exposures from 01:23-04:39 UT on May 28 (Fig. 1), beginning ~3 hours after the eruption onset (Table 1). The sequence of EPIC images (Fig. 1) reveals slow movement of the SO_2 cloud away from the volcano over ~3 hours, indicating low wind speeds (consistent with the closest available radiosonde sounding; Fig. S1) and consequently low wind shear. Since high wind shear could reduce SO_2 columns below the EPIC detection limit, these conditions are favorable for geophysical interpretation of SO_2 mass variations.

Coincident thermal IR data from the GOES-15 (GOES-W) satellite show ~N-NE transport of an opaque volcanic cloud (Fig. 1, Fig. S2). Geostationary satellite data suffer from parallax effects (e.g., *Johnson et al.,* 1994) that displace objects away from the sub-

satellite point (135ºW for GOES-W), but we have corrected for this in Figure 2 using a normalized cloud offset (http://www-das.uwyo.edu/~geerts/cwx/notes/chap02/parallax.html). For a cloud at 11-15 km altitude and 54ºN, the parallax offset is ~20-30 km, which we confirmed by comparing a visible SNPP/VIIRS (LEO) image of the volcanic cloud at 23:35 UTC with the uncorrected GOES-W image at 23:30 UTC. Note that whilst EPIC also suffers from parallax effects, they are negligible in this case due to DSCOVR's much greater distance from Earth and the northern hemisphere location of the sub-satellite point in late May (close to the summer solstice). The parallax-corrected GOES-W data and near-coincident EPIC SO_2 retrievals (Fig. 1) reveal a clear separation of the hydrometeor/ash and SO_2-rich portions of the volcanic cloud, with the SO_2 at higher altitude (since it is not obscured by the opaque cloud). Radiosonde data (Fig. S1) suggests an altitude of 12-13 km for the SO_2 cloud. *Rose et al.* (2000) speculated on several mechanisms to explain this separation of ash and gas in volcanic clouds, including dynamic separation, pre-eruptive gas segregation, or SO_2 scavenging. The Bogoslof data show EPIC's potential to provide more observational constraints on this phenomenon and elucidate the processes involved (e.g., in conjunction with plume modeling; *Prata et al.*, 2017).

The EPIC SO_2 data for Bogoslof also reveal a transient SO_2 feature in the 02:28 UT exposure, distinct from the main SO_2 cloud and the opaque cloud detected by GOES-W (Fig. 1b). Release of SO_2 from sublimating ice (e.g., *Textor et al*., 2003) or oxidation of H_2S are potential sources for this transient gas. Possible sources of H_2S in the Bogoslof emissions include magmatic gas (e.g., *Aiuppa et al.*, 2005) or magma-water interactions in the aqueous environment of the vent (e.g., *Clarisse et al.*, 2011) . The rate constant for reaction of the OH radical with H_2S is an order of magnitude larger than its reaction with SO_2, hence oxidation of H_2S to SO_2 should proceed more rapidly than conversion of SO_2 to sulfate aerosol (e.g., Graedel, 1977; Rose et al., 2000). We also note that SNPP/OMPS measured ~7-8 kt of SO_2 in

the Bogoslof volcanic cloud ~19 hours later on May 29 at 23:15-23:20 UT (Fig. S3), indicating no significant SO_2 loss on this timescale. This would be consistent with production of SO_2 (e.g., via oxidation of H_2S) dominating (or compensating for) SO_2 loss during this period.

4.2 The October 20, 2017 eruption of Tinakula (Solomon Islands)

The October 2017 eruption of remote Tinakula volcano was relatively small (VEI ~3), yet among the largest eruptions of that year. The eruption consisted of two explosive events: the first began at around 19:20 UT on October 20, injecting an ash plume to 4.6 km altitude, followed by a second ash-producing eruption at 23:40 UT that reached 10.7 km altitude and generated a visible shock wave (*Global Volcanism Program*, 2017). EPIC detected SO_2 emissions from the first eruption at 20:53 UT on October 20, less than 2 hours after the onset (Table 1; Fig. 2), and the subsequent EPIC exposure (22:41 UT) measured ~14 kt of SO_2 in the eruption cloud. The next EPIC measurement (00:55 UT, Oct 21) occurred ~80 minutes after the second explosive event (when we assume some residual SO_2 from the first eruption remained), but did not detect an increase in SO_2 loading (Fig. 2). At ~02:20 UT overpasses of the LEO UV sensors (OMI and OMPS) measured the merged SO_2 loading from both eruptive events, which were also observed in later EPIC exposures but which remained below the ~14 kt measured at 22:41 UT on October 20 (Fig. 2). Thus in this case the EPIC observations permit distinction between emissions from two separate eruptions, indistinguishable in the LEO data, and suggest that the first eruptive event likely discharged most of the SO_2. Such attribution of gas emissions during eruptions with multiple phases is important for understanding volcanic processes such as pre-eruptive gas accumulation.

The lower SO_2 sensitivity of EPIC relative to hyperspectral LEO UV sensors such as OMI is apparent in Figure 2. OMI measured a higher total SO_2 loading at 02:23 UT (~20 kt)

than EPIC at 02:43 UT (~11 kt), since EPIC lacks sensitivity to the lower SO_2 columns near the periphery of the volcanic cloud (Fig. 2). However, the comparison shows that the EPIC retrievals are in good agreement (in terms of location and SO_2 column) with OMI in the core of the SO_2 cloud and provide important context for the LEO observations. We reiterate that the 2017 Tinakula eruption was relatively small and we expect EPIC to provide optimal data when the next major stratospheric volcanic eruption occurs.

4.3 The June 2018 eruption of Sierra Negra (Galápagos Islands, Ecuador)

Two Galápagos Island eruptions in June 2018 provided the best demonstration yet of the advantages of high-cadence EPIC observations. Fernandina volcano (Isla Fernandina) began a short (2-3 day) eruption on June 16, 2018, then Sierra Negra (Isla Isabela) erupted on June 26, continuing into July. Both eruptions were captured in 7-9 consecutive EPIC exposures (Table 1) due to the favorable Equatorial location. We focus here on the Sierra Negra eruption, but animations of EPIC SO_2 data for both events are provided as supplementary material (Supplementary Movies S1, S2 and S3). Both eruptions were predominantly effusive events with low VEIs of 1-2 (*Global Volcanism Program*, 2013).

The Sierra Negra eruption began at 19:40 UT on June 26, and an SNPP/OMPS overpass ~30 minutes later at 20:09 UT measured a small amount of SO_2 (~0.5 kt); though insufficient to be deemed a significant eruption. However, a late afternoon EPIC exposure at 21:57 UT detected high SO_2 column amounts (~90 DU) southwest of the volcano (Fig. 3), indicative of a significant eruption in progress. On June 27, EPIC observations were available at peak hourly cadence and the Sierra Negra SO_2 cloud was detected in 8-9 consecutive exposures (Fig. 3; Supplementary Movie S2), which is probably the maximum achievable. Figure 4b shows the cumulative SO_2 amount detected in these exposures, and nicely captures the curved trajectory of a parcel of SO_2 transported to the south. We attempted to fit HYbrid

Single Particle Lagrangian Integrated Trajectory (HYSPLIT) model (*Stein et al*., 2015; *Rolph et al*., 2017) trajectories to the EPIC SO_2 data. Trajectories initialized over Sierra Negra at 19:00 UT on June 26 at altitudes of 11-13 km provided the best match with SO_2 detected by EPIC southwest of the volcano (Fig. 3b); discrepancies may be due to insufficient meteorological data driving the HYSPLIT model in the region. SO_2 loadings measured in the consecutive EPIC exposures on June 27 shows a steady decline over the ~8-hour period from ~55 kt at 14:38 UT to ~27 kt at 22:16 UT (Supplementary Movie S2). Most of this variation is probably due to changing SO_2 sensitivity as the EPIC viewing geometry and solar zenith angle (SZA) changes, but it is clear that there were no further significant SO_2 emissions from Sierra Negra in this timeframe. Hence, unlike LEO sensors, the EPIC observations can potentially provide information on hourly trends in eruption intensity, although this will require further analysis of how sensitivity varies with observation geometry.

In Figure 3 we also show a SNPP/OMPS SO_2 measurement using the Principal Component Analysis (PCA) algorithm (*Li et al*., 2017) made close to the time of one EPIC exposure. As for Tinakula, this shows the lower sensitivity of EPIC relative to the hyperspectral UV instruments, but nevertheless demonstrates the consistency between EPIC and OMPS SO_2 columns in the core region of the volcanic cloud. And unlike the single OMPS SO_2 image, the sequence of EPIC observations provides unique information on cloud transport and short-term trends in eruption intensity (Fig. 3; Supplementary Movie S2, S3).

5. Discussion

Our results demonstrate that EPIC has sufficient SO_2 sensitivity (~5-10 DU) to detect all significant volcanic eruptions that occur within its field-of-view (FOV). However, EPIC's unique advantage over LEO satellite instruments is the higher cadence of SO_2 observations. Continuous eruptions (e.g., Sierra Negra in June 2018), or eruptions that begin as the volcano

rotates into the EPIC FOV, will yield the maximum number of daily EPIC observations, albeit with varying SZA. The Galápagos Islands eruptions in June 2018 (Table 1) show that at least 7-8 EPIC exposures over a period of several hours can be obtained, potentially revealing short-term trends in volcanic emissions. Future work will quantify the impact of varying observing conditions (e.g., SZA) on EPIC's SO_2 detection limit and retrieval uncertainties.

EPIC offers the potential for rapid detection of eruptions within its FOV, and for assessment of eruption evolution on hourly timescales, which would be advantageous for volcanic hazard mitigation. EPIC currently has no near real-time (NRT) data capability as only two antennae (in Virginia and Alaska, USA) are used for downlink to Earth, and only receive data when in view of DSCOVR (*Herman et al.*, 2018). This could be remedied by installation of more receivers, such that at least one antenna is always within the EPIC FOV. But regardless of NRT capabilities, early detection of volcanic clouds is critical for accurate assessment of eruptive SO_2 emissions, particularly for major eruptions with potential climate impacts. LEO UV sensors often detect volcanic eruptions several hours, or close to a day, after the eruption onset, during which time the emitted SO_2 mass can change substantially. LEO SO_2 measurements can be extrapolated back to the time of eruption (e.g., *Krotkov et al.*, 2010), but this requires a long time-series of SO_2 loadings that takes days to weeks to acquire. As shown here, EPIC has detected several eruptions within a few hours of their onset, and despite lower sensitivity than hyperspectral UV sensors EPIC's higher cadence provides context for LEO SO_2 measurements and allows us to gauge how representative the LEO data might be of the peak volcanic SO_2 loading. EPIC SO_2 observations would therefore also be of value for assimilation into climate models that predict volcanic impacts on climate.

6. Conclusions

The DSCOVR/EPIC instrument, in orbit at L1 since 2015, is a valuable addition to current space-borne assets capable of detecting volcanic eruption clouds, providing unique UV observations of volcanic SO_2 with hourly cadence. Results presented here show that our EPIC SO_2 algorithm has detected every significant volcanic eruption since the DSCOVR launch. Although relatively small, these eruptions have demonstrated EPIC's sensitivity to moderate volcanic eruptions at a range of latitudes. EPIC should provide exceptional observations if still operational when the next major stratospheric volcanic eruption (VEI 4+) occurs. We have also demonstrated EPIC's ability to track volcanic cloud transport on hourly timescales; a significant advance over LEO UV sensors (e.g., OMI, OMPS). Preliminary comparisons of EPIC SO_2 retrievals with OMI and OMPS data indicate consistent SO_2 columns and loadings. It is clear that the EPIC observations have great potential to provide new insight into the short-term evolution of volcanic SO_2 clouds, and also to enable more timely detection of volcanic eruptions. The potential value of frequent UV observations of volcanic clouds has been noted in the past, and with EPIC this has become a reality.

Acknowledgments

We acknowledge NASA Earth Science Division support for development of the EPIC SO_2 products through grant NNX15AC61G (DSCOVR Earth Science Algorithms program; PI: N.A. Krotkov). EPIC Sulfur Dioxide data products are available at the Atmospheric Science Data Center (ASDC) at NASA Langley Research Center: https://eosweb.larc.nasa.gov/project/dscovr/dscovr_epic_l2_so2_01. The NOAA Air Resources Laboratory (ARL) is acknowledged for the provision of the HYSPLIT transport and dispersion model and/or READY website (http://www.ready.noaa.gov) used in this publication.

References

Aiuppa, A., S. Inguaggiato, A.J.S. McGonigle, M. O'Dwyer, C. Oppenheimer, M.J. Padgett, D. Rouwet, and M. Valenza (2005), H_2S fluxes from Mt. Etna, Stromboli, and Vulcano (Italy) and implications for the sulfur budget at volcanoes, *Geochim. Cosmochim. Acta*, 69(7), 1861-1871, doi:10.1016/j.gca.2004.09.018.

Carn, S.A., L. Clarisse and A.J. Prata (2016), Multi-decadal satellite measurements of global volcanic degassing, *J. Volcanol. Geotherm. Res.*, 311, 99-134, http://dx.doi.org/10.1016/j.jvolgeores.2016.01.002.

Clarisse, L., P.-F. Coheur, S. Chefdeville, J.-L. Lacour, D. Hurtmans, and C. Clerbaux (2011), Infrared satellite observations of hydrogen sulfide in the volcanic plume of the August 2008 Kasatochi eruption, *Geophys. Res. Lett*., 38, L10804, doi:10.1029/2011GL047402.

Graedel, T.E. (1977), The homogenous chemistry of atmospheric sulfur, *Rev. Geophys.*, 15, 421-428.

Global Volcanism Program (2013), Volcanoes of the World, v. 4.7.4. Venzke, E (ed.). Smithsonian Institution. Downloaded 04 Oct 2018. https://doi.org/10.5479/si.GVP.VOTW4-2013

Global Volcanism Program (2017), Report on Tinakula (Solomon Islands). In: Sennert, S K (ed.), Weekly Volcanic Activity Report, 18 October-24 October 2017. Smithsonian Institution and US Geological Survey.

Global Volcanism Program (2018), Report on Fuego (Guatemala). In: Sennert, S K (ed.), Weekly Volcanic Activity Report, 30 May-5 June 2018. Smithsonian Institution and US Geological Survey.

Herman, J., Huang, L., McPeters, R., Ziemke, J., Cede, A., and Blank, K. (2018), Synoptic ozone, cloud reflectivity, and erythemal irradiance from sunrise to sunset for the

whole Earth as viewed by the DSCOVR spacecraft from the Earth-Sun Lagrange 1 orbit, *Atmos. Meas. Tech*., 11, 177-194, https://doi.org/10.5194/amt-11-177-2018.

Johnson, D. B., P. Flament and R.L. Bernstein (1994), High-resolution satellite imagery for mesoscale meteorological studies. *Bull. Amer. Meteor. Soc*., 75, 5-33.

Krotkov, N.A., M.R. Schoeberl, G.A. Morris, S.A. Carn, and K. Yang (2010), Dispersion and lifetime of the SO_2 cloud from the August 2008 Kasatochi eruption, *J. Geophys. Res*., 115, D00L20, doi:10.1029/2010JD013984.

Krueger, A.J., Walter, L.S., Bhartia, P.K., Schnetzler, C.C., Krotkov, N.A., Sprod, I., Bluth, G.J.S. (1995), Volcanic sulfur dioxide measurements from the total ozone mapping spec- trometer instruments. *J. Geophys. Res*. D100, 14057–14076.

Krueger, A.J., Schaefer, S.J., Krotkov, N., Bluth, G., Barker, S. (2000), Ultraviolet remote sens- ing of volcanic emissions. In: Mouginis-Mark, P.J., Crisp, J.A., Fink, J.H. (Eds.), Remote Sensing of Active Volcanism, *Geophysical Monograph* 116. AGU, Washington, DC, pp. 25–43.

Li, C., N.A. Krotkov, S.A. Carn, Y. Zhang, R.J.D. Spurr, and J. Joiner (2017), New-generation NASA Aura Ozone Monitoring Instrument volcanic SO_2 dataset: Algorithm description, initial results, and continuation with the Suomi-NPP Ozone Mapping and Profiler Suite, *Atmos. Meas. Tech*., 10, 445-458, doi:10.5194/amt-10-445-2017.

Marshak, A., et al. (2018), Earth observations from DSCOVR/EPIC instrument, *Bulletin American Meteorol. Soc.*, doi: 10.1175/BAMS-D-17-0223.1, in press.

Pavolonis, M., A. Heidinger, and J. Sieglaff (2013), Automated retrievals of volcanic ash and dust cloud properties from upwelling infrared measurements, *J. Geophys. Res.*, 118, 1436–1458, doi:10.1002/jgrd.50173.

Prata, A. J., and J. Kerkmann (2007), Simultaneous retrieval of volcanic ash and SO_2 using MSG-SEVIRI measurements, *Geophys. Res. Lett*., 34, L05813, doi:10.1029/2006GL028691.

Prata, F., Woodhouse, M., Huppert, H. E., Prata, A., Thordarson, T. and Carn, S. (2017), Atmospheric processes affecting the separation of volcanic ash and SO_2 in volcanic eruptions: inferences from the May 2011 Grímsvötn eruption, *Atmos. Chem. Phys*., 17, 10709–10732.

Rolph, G., Stein, A., and Stunder, B. (2017), Real-time Environmental Applications and Display sYstem: READY. *Environmental Modelling & Software*, 95, 210-228, https://doi.org/10.1016/j.envsoft.2017.06.025.

Rose, W.I., G.J.S. Bluth, and G.G.J. Ernst (2000), Integrating retrievals of volcanic cloud characteristics from satellite remote sensors: a summary, *Phil. Trans. R. Soc. Lond. A.*, 358, 1585-1606.

Stein, A.F., Draxler, R.R, Rolph, G.D., Stunder, B.J.B., Cohen, M.D., and Ngan, F. (2015), NOAA's HYSPLIT atmospheric transport and dispersion modeling system, *Bull. Amer. Meteor. Soc*., 96, 2059-2077, http://dx.doi.org/10.1175/BAMS-D-14-00110.

Textor, C., H.-F. Graf, M. Herzog, and J. M. Oberhuber (2003), Injection of gases into the stratosphere by explosive volcanic eruptions, *J. Geophys. Res.*, 108(D19), 4606, doi:10.1029/2002JD002987.

Table 1. Volcanic eruptions detected by EPIC (June 2015 – July 2018)

Volcano	Eruption time (UTC)	First EPIC detection (UTC)	Difference (hours)[1]	EPIC exposures[2]	Maximum SO_2 column (DU)
Etna (Italy)	Dec 3, 2015, 02:30	Dec 3, 08:16	5.77	3	46
Bromo (Indonesia)	Jan 2, 2016	Jan 2, 04:09	-	3	38
Pavlof (USA)	Mar 27, 2016, 23:53	Mar 28, 21:54	22.02	2	25
Aso-san (Japan)	Oct 7, 2016, 16:46	Oct 8, 00:55	8.15	4	33
Bogoslof (USA)	Mar 8, 2017, 07:36	Mar 8, 20:15	12.65	3	29
Kambalny (Russia)	Mar 24, 2017, 21:20	Mar 25, 02:43	5.38	4	18
Bogoslof (USA)	May 28, 2017, 22:16	May 29, 01:23	3.12	4	38
Tinakula (Solomon Is)	Oct 20, 2017, 19:20	Oct 20, 20:53	1.55	5	68
Agung (Indonesia)	Nov 26, 2017	Nov 27, 03:53	-	1	28
Sinabung (Indonesia)	Feb 19, 2018, 01:53	Feb 19, 03:53	2	4	74
Ambae (Vanuatu)	Mar 24, 2018	Mar 24, 00:55	-	3	82
Ambae (Vanuatu)	Apr 6, 2018	Apr 6, 01:04	-	3	71
Fuego (Guatemala)	Jun 3, 2018, 17:30[3]	Jun 3, 18:03[4]	0.55	3	37
Fernandina (Ecuador)	Jun 16, 2018, 17:00	Jun 16, 19:28	2.47	7	44
Sierra Negra (Ecuador)	Jun 26, 2018, 19:40	Jun 26, 21:57	2.28	8-9	91
Ambae (Vanuatu)	Jul 26, 2018 10:00	Jul 26, 20:24	10.4	4	221

1. Only given if eruption start time is known.
2. Maximum number of consecutive EPIC exposures containing volcanic SO_2.
3. Onset of largest explosive eruption as reported by the Washington Volcanic Ash Advisory Center (VAAC; Global Volcanism Program, 2018).
4. Aerosol Index (AI) signal indicating volcanic ash.

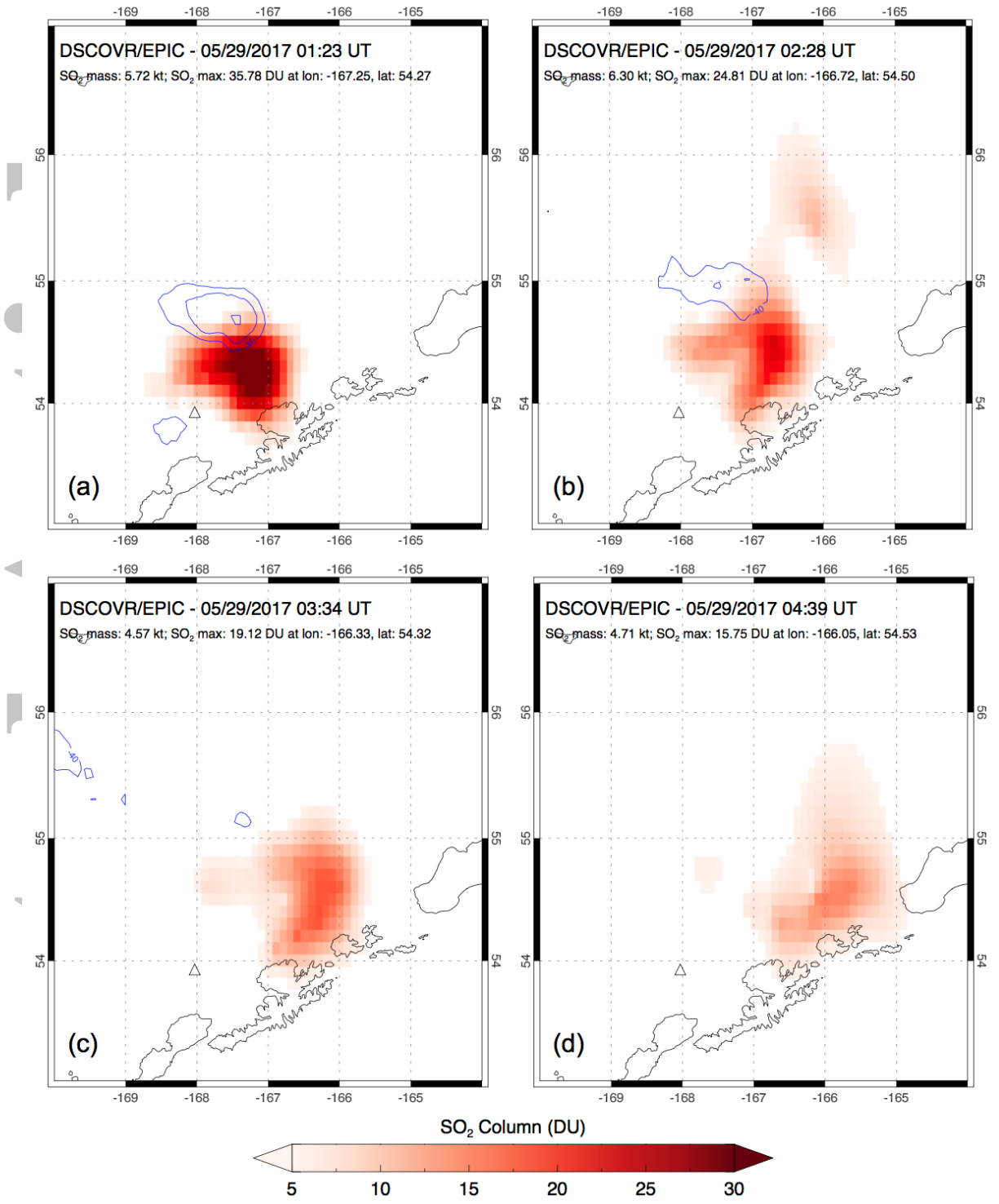

Figure 1. Four consecutive EPIC SO_2 maps for the May 28-29, 2017 eruption of Bogoslof volcano (AK, USA; *triangle*). The eruption occurred at 22:16 UTC on May 28 (Table 1). SO_2 in the Bogoslof volcanic cloud was detected in four EPIC exposures on May 29 at (a) 01:23 UTC; (b) 02:38 UTC; (c) 03:34 UTC; and (d) 04:39 UTC. The EPIC retrievals show the relatively slow movement of the SO_2 cloud to the northeast. The *blue contours* shown in (a)-(c) denote regions of IR brightness temperatures ≤-40ºC derived from near-coincident GOES-15 geostationary infrared data. These demarcate the boundary of an opaque, ice-rich volcanic cloud (likely also containing ash) which is separate from (below) the SO_2 cloud.

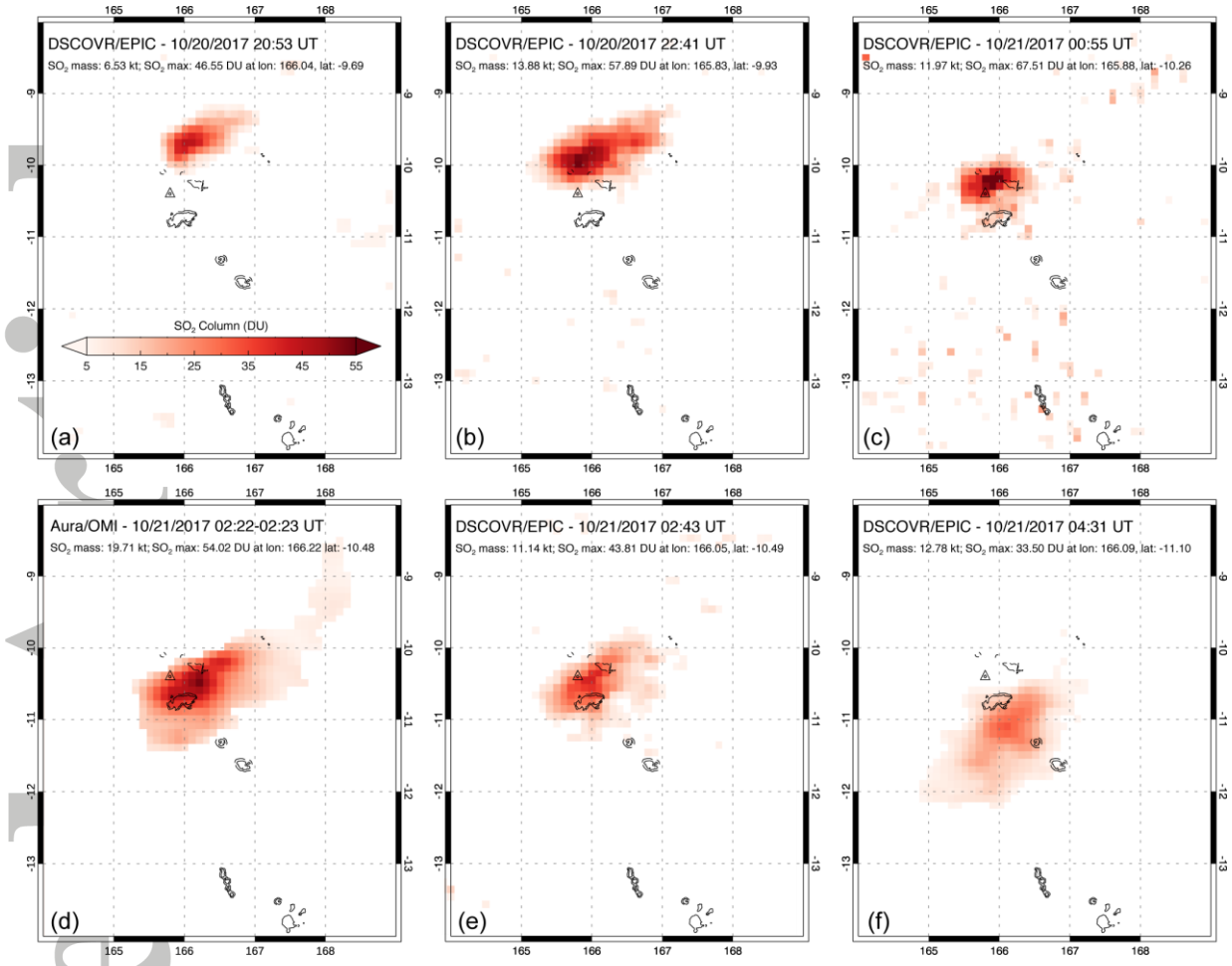

Figure 2. Five consecutive EPIC SO_2 images for the October 20-21, 2017 eruption of Tinakula volcano (Solomon Islands; *triangle*). Two separate eruptions occurred at 19:20 and 23:40 UT on October 20 (Table 1). SO_2 was detected in EPIC exposures at (a) 20:53 UTC Oct 20; (b) 22:41 UT Oct 20; (c) 00:55 UT Oct 21; (e) 02:43 UT Oct 21; and (f) 04:31 UT Oct 21. All EPIC images use the color scale shown in (a). Panel (d) shows a LEO Aura/OMI Principal Component Analysis (PCA) algorithm SO_2 retrieval (*Li et al.*, 2017) at 02:23 UT on Oct 21, using the same color scale as the EPIC maps.

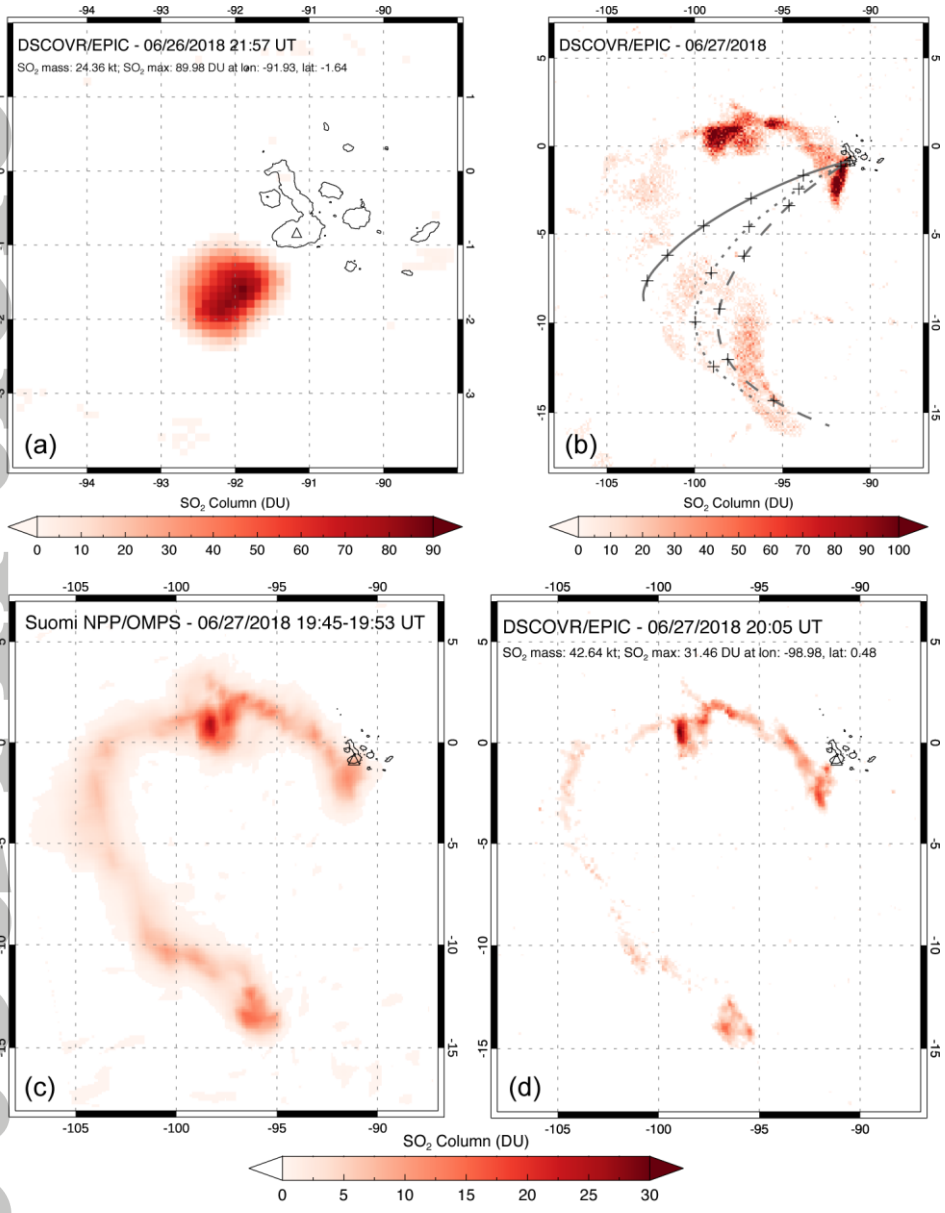

Figure 3. (a) EPIC detection of strong SO_2 emissions from Sierra Negra (Galápagos Islands; *triangle*) at 21:57 UT on June 26, 2018; (b) Cumulative SO_2 column amounts measured in the Sierra Negra volcanic plume by EPIC in 8 exposures on June 27, 2018 (14:38-22:16 UT). *Dashed, dotted and solid lines* show 36-hour HYSPLIT model forward trajectories for an eruption to altitudes of 11, 12 and 13 km, respectively, beginning at 19:00 UT on June 26, with *crosses* every 6 hours. (c) SNPP/OMPS map of SO_2 emissions from Sierra Negra at 19:50 UT on June 27 (maximum SO_2 column is 27 DU); (d) EPIC SO_2 map at 20:05 UT on June 27 (maximum SO_2 column is 31 DU). Panels (c) and (d) use the same color scale.